Experimental study on reinforced high-strength concrete short columns confined with AFRP sheets

Han-Liang Wu[1,2] and Yuan-Feng Wang[*1]

[1]*School of Civil Engineering, Beijing Jiaotong University, Beijing, 100044, China*
[2]*Bridge Technology Research Center, Research Institute Center of Highway, Ministry of Transportation, Beijing, 100088, China*

Abstract. This paper is aiming to study the performances of reinforced high-strength concrete (HSC) short columns confined with aramid fibre-reinforced polymer (AFRP) sheets. An experimental program, which involved 45 confined columns and nine unconfined columns, was carried out in this study. All the columns were circular in cross section and tested under axial compressive load. The considered parameters included the concrete strength, amount of AFRP layers, and ratio of hoop reinforcements. Based on the experimental results, a prediction model for the axial stress-strain curves of the confined columns was proposed. It was observed from the experiment that there was a great increment in the compressive strength of the columns when the amount of AFRP layers increases, similar as the ultimate strain. However, these increments were reduced as the concrete strength increasing. Comparisons with other existing prediction models present that the proposed model can provide more accurate predictions.

Keywords: high-strength concrete (HSC); reinforced concrete column; aramid fibre-reinforced polymer (AFRP); experiment; prediction model.

1. Introduction

In recent years, fibre-reinforced polymer (FRP) material has been used to strengthen and repair concrete structures successfully. One of most efficient applications is wrapping concrete columns with FRP sheets. Concrete columns confined with FRP sheets can get higher stiffness and strength, and better durability than unconfined ones (Mirmiran 1997, Samaan 1998, Saafi *et al*. 1999, Xiao and Wu 2000, Fam and Rizkalla 2001, Karabinis and Rousakis 2002, Teng and Lam 2004). Most of the previous studies focused on plain concrete short columns and normal-strength concrete (NSC) short columns. However, in practice, high-strength concrete (HSC) has gotten wide application in civil engineering for its predominant strength performance, but its use is limited by a concern regarding an increased brittleness compared to NSC. It has been demonstrated that the ductility of HSC columns can be enhanced by external confinement (Tabsh 2007), attributed to hoop reinforcements or FRP wrapping.

For NSC columns confined with both spiral and carbon FRP (CFRP), Li *et al*. (2002, 2003) developed an empirical model to predict the compressive strength of the columns based on the Mohr-Columb failure envelope theory, and concluded that different types of hoop reinforcements had very little effect

---

* Corresponding author, Proffessor, E-mail: cyfwang@bjtu.edu.cn

on the compressive strength. Lin and Liao (2003) tested the compressive strength of plain concrete and reinforced concrete (RC) columns confined by glass FRP (GFRP), the results indicated that the GFRP's confinements for the two types of columns were similar, and the method for analyzing the behavior of FRP-confined plain concrete columns could be also adapted to those of FRP-confined RC columns. Based on the assumption that the total compressive strength was equal to the sum of three components (the benefits from concrete, reinforced bars and FRP), they proposed a theoretical model for the axial stress-strain curves of the columns, which agreed with the experimental data well. Mortazavi *et al.* (2003) experimental investigated the performances of RC columns confined by pre-tensioned FRP, it was shown that the RC columns confined by pre-tensioned FRP (including CFRP, GFRP) could increase their load carrying capacity up to 35% compared with those without pre-tensioned. Lin *et al.* (2006), Yeh and Chang (2007) simulated the compressive behavior of FRP-confined concrete columns by means of finite element method. Additionally, several researchers reported their studies on plain HSC columns confined with FRP sheets. Li (2006) investigated the influence of confinement efficiency to HSC cylinders confined with GFRP. He found that the insufficiently confined cylinders behaved similar to the plain cylinders, and also pointed out that there was a considerable deviation between the predictions by existing design-oriented models and experimental data. Almusallam (2007) studied HSC cylinders confined with GFRP, it was observed that the increments in compressive strength and ductility of confined HSC columns was less than that of confined NSC columns which were wrapped a same amount of FRP sheets.

In addition, most of the previous researches focused on concrete columns confined with CFRP and GFRP, works on those confined with aramid FRP (AFRP) are rather little. In fact, AFRP is different from CFRP and GFRP in properties of strength, elastic modulus, ultimate rupture strain, durability and so on. For instances, although the tensile strength of AFRP is 20% lower than that of CFRP, the elongation-to-break of AFRP is 60% higher than that of CFRP. Compared with GFRP, AFRP has slightly higher elongation-to-break, but higher strength. Thus, reinforced HSC columns confined with AFRP maybe have different performance from those confined with CFRP and GFRP, and some further studies on this kind of columns are necessary.

The objectives of this paper are as follows: (1) present the experimental investigation and results; (2) propose a prediction model for the axial stress-strain curves of reinforced HSC circular columns confined with AFRP sheets under axial compressive load; (3) make comparisons between the experimental results and values from the proposed model and two typical existing models, in order to verify the proposed model.

2. Experiment procedures

2.1 Specimens preparation

Three sets of specimens, consisting of 18 types of specimens (three of each type), were conducted. The following parameters were considered in the experiments: (1) the concrete strength: three grades of concrete strengths were tested, $f_{c0} = 46.43$, 78.50, and 101.18 MPa, respectively; (2) the amount of AFRP layers: the specimens confined with one, two and three layers of AFRP sheets were investigated; (3) the ratio of hoop reinforcements: two types of hoops with diameters of 4 mm (the yield strength of hoop reinforcements $f_{yv} = 265$ MPa, the elastic modulus of hoop reinforcements $E_{sv} = 2 \times 10^5$ MPa) and 6 mm ($f_{yv} = 260$ MPa , $E_{sv} = 2 \times 10^5$ MPa), respectively. Each type of the RC specimen was referred

Table 1 Summaries of specimens and experimental results

Specimen designation	d_{sv} (mm)	Confinement ratio of transverse hoop ($f_{l,s}/f_{c0}$)	n_f	Confinement ratio of AFRP ($f_{l,f}/f_{c0}$)	f_{cc} (MPa)	$\dfrac{f_{cc}-f_{c0}}{f_{c0}}$	$\varepsilon_{cc1}(\times 10^{-3})$	$\dfrac{\varepsilon_{cc1}-\varepsilon_{c0}}{\varepsilon_{c0}}$
L-C	-	0.000	0	0.000	46.43	0.00	2.55	0.00
L-d4-1	4	0.041	1	0.254	113.91	1.45	16.73	5.56
L-d4-2	4	0.041	2	0.508	163.74	2.53	26.66	9.45
L-d4-3	4	0.041	3	0.761	194.71	3.19	27.40	9.75
M-C	-	0.000	0	0.000	78.50	0.00	4.51	0.00
M-d4-1	4	0.024	1	0.150	133.84	0.70	14.73	5.02
M-d4-2	4	0.024	2	0.300	188.66	1.40	21.15	6.33
M-d4-3	4	0.024	3	0.450	215.16	1.74	27.58	7.36
M-d6-1	6	0.054	1	0.150	152.01	0.94	19.46	3.55
M-d6-2	6	0.054	2	0.300	197.45	1.52	25.89	4.46
M-d6-3	6	0.054	3	0.450	217.13	1.77	32.31	6.53
H-C	-	0.000	0	0.000	101.18	0.00	4.56	0.00
H-d4-1	4	0.019	1	0.116	142.03	0.40	12.62	1.24
H-d4-2	4	0.019	2	0.233	193.33	0.91	17.69	5.30
H-d4-3	4	0.019	3	0.349	247.54	1.45	22.71	5.29
H-d6-1	6	0.042	1	0.116	160.00	0.58	16.29	3.68
H-d6-2	6	0.042	2	0.233	208.29	1.06	21.36	6.35
H-d6-3	6	0.042	3	0.349	234.86	1.32	26.38	7.75

with a plain specimen. A summary of the specimens is presented in Table 1.

The dimension of specimens was uniform (as shown in Fig. 1), 100 mm in diameter, 300 mm in height, and the diameter of longitudinal reinforcement in RC specimens was 8 mm (the yield strength of longitudinal bars $f_y = 260$ MPa, the elastic modulus of longitudinal bars $E_s = 2 \times 10^5$ MPa). All the specimens were cured for 28 days at a temperature of $20 \pm 2°$C and a relative humidity that exceeded 95%. Then, excepting the nine controlled specimens, the specimens were wrapped with different amount of AFRP sheets, and special attention was paid to that an extended overlayer of 100 mm was applied, in order to ensure the development of composite's strength. All the specimens were left for at least seven days before testing. The mechanical properties of AFRP composites used is presented in Table 2.

2.2 Instrumentation and loading

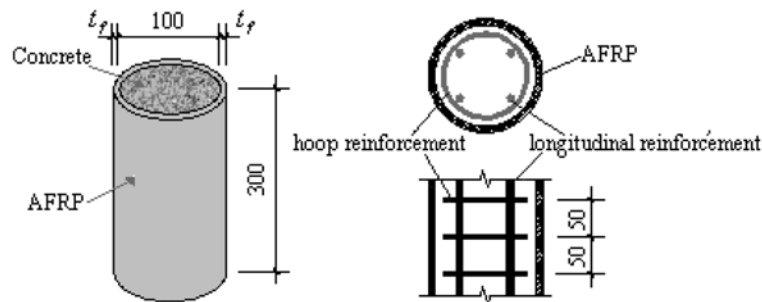The axial deformations were measured by an electronic extensometer. All the specimens were tested

Fig. 1 The dimension of specimen and location of reinforcement

Table 2 Mechanical properties of AFRP materials

Standard of AFRP	f_f (MPa)	E_f (GPa)	t_f (mm)	ε_{fu}
AFS-60	2060	118	0.286	1.77%

by using a compression machine (3000 kN capacity), and the experimental data were monitored through an automatic data acquisition system. All specimens were tested to failure under a monotonically increasing concentric load, and the loading control mode was 0.15 MPa/sec in stress, then changed to 0.001 ε / s in strain after exceeding 80% of the unconfined concrete compressive strength.

2.3 Results

The failure started at the middle height of the specimens with some noisy sounds during the early and middle stages of loading, which may be caused by the microcracking of concrete, or shifting of aggregates, or breaking of resins possibly. Near the end of loading process, snapping of inner layers of AFRP could be heard. With sudden explosion, AFRP sheets were broken, and the specimens failed completely with lots of crushed concrete. The longitudinal bars were buckling. In some cases, the hoop reinforcements were broken (as shown in Fig. 2).

Table 1 presents the observed experimental data. Each value of the compressive strength (f_{cc}) or the ultimate strain (ε_{cc1}) was the average of each type of specimens. The experimental results show that the compressive strength and the ultimate strain of confined specimens are both increased notably. The improvement of compressive strength is between 145% and 319% for the specimens of f_{c0} = 46.43 MPa, between 70% and 177% for f_{c0} = 78.50 MPa, and between 40% and 145% for f_{c0} = 101.18 MPa. The increment of ultimate strain is between 556% and 975%, 355% and 736%, 124% and 775% for the specimens of f_{c0} = 46.43, 78.50, and 101.18 MPa, respectively. However, for the same grade of concrete strength, there are more increments with more amount of AFRP wrapping or bigger ratio of hoop reinforcements. When the same amount of AFRP applied, the increments are reduced relatively as the strength of concrete increasing (as shown in Fig. 3), because HSC is more brittleness as its strength increasing. It demonstrates that the increment on compressive strength due to the AFRP is more efficient when the strength of concrete is relatively lower.

Shown in Fig. 4 are the experimental stress-strain curves of the specimens. All the stress-strain curves
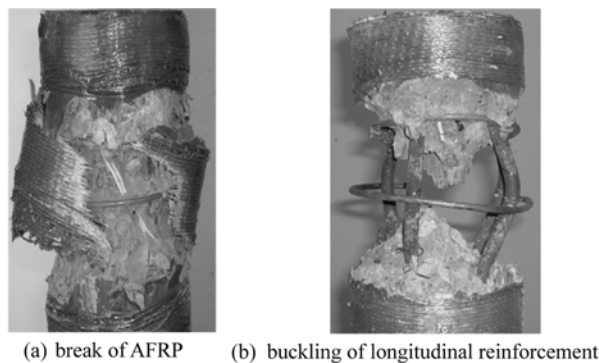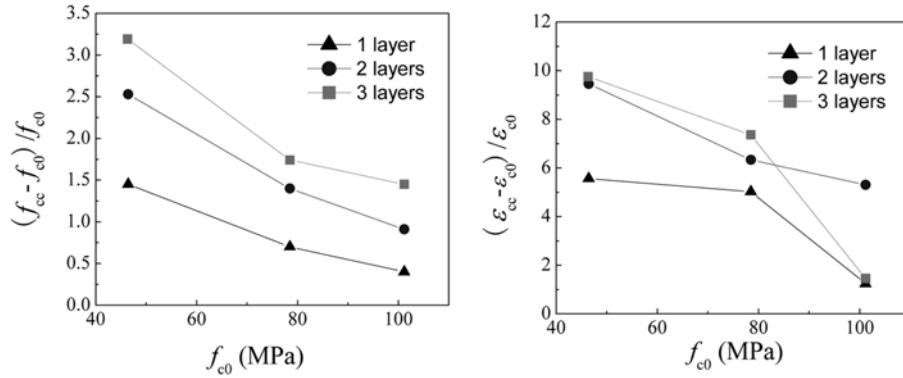

(a) break of AFRP   (b) buckling of longitudinal reinforcement

Fig. 2 Failure modes of the specimens

Fig. 3 Increments of compressive strength and ultimate strain (d_{sv} = 4 mm)

(a) f_{c0}=46.43MPa, d_{sv}=4mm

(b) f_{c0}=78.50MPa, d_{sv}=4mm

(c) f_{c0}=101.18MPa, d_{sv}=4mm

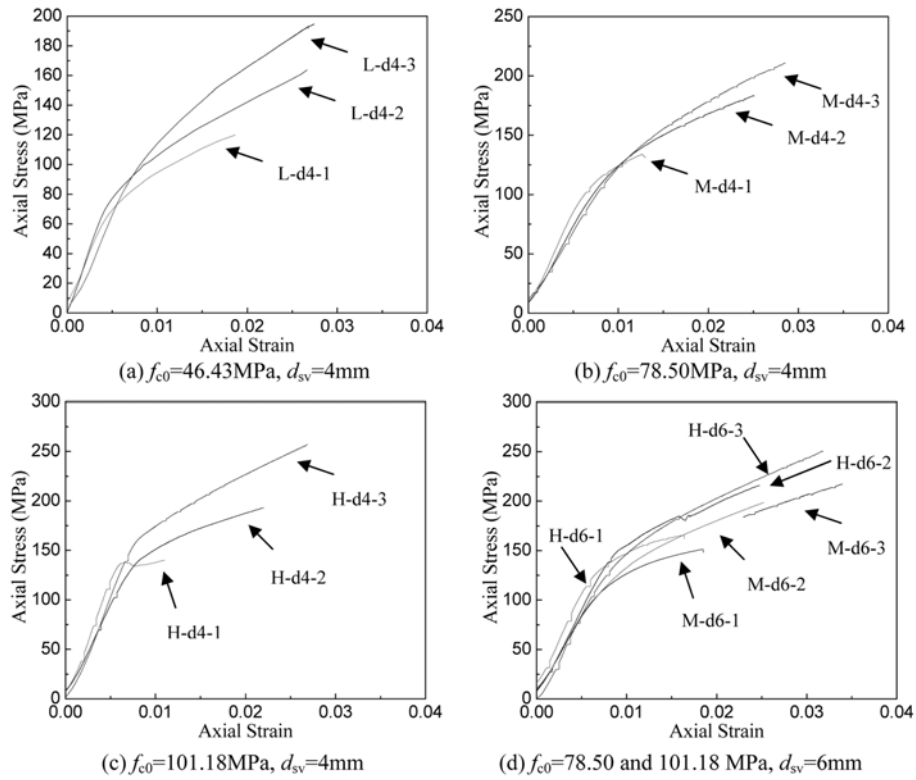(d) f_{c0}=78.50 and 101.18 MPa, d_{sv}=6mm

Fig. 4 Shape of experimental stress-strain curves

are bilinear, and can be separated into two stages with a transition zone. In the first stage, the curves ascend with slopes almost equal to that of the plain concrete, until reaching the unconfined concrete strength. It shows that confinements of AFRP and hoop reinforcements have insignificant effects on the elastic modulus of the columns, because of little dilation in lateral direction. Then, in the second stage, the curves continue to ascending, but the slopes would be reduced. The reductions of slopes are depending on the amount of AFRP sheets and the concrete strength.

3. Prediction models

Using experimental data and/or some failure theory, various models have been developed to predict the stress-strain curves of columns confined with FRP or hoop reinforcements. In this section, a model based on the experimental results is presented to predict the behavior of reinforced HSC columns confined with AFRP sheets. For a sake of comparison, two typical existing prediction models are selected: (1) The Lokuge's model (Lokuge *et al.* 2005), which was developed based on the experimental data of confined plain HSC columns, and was proved to be generally in close agreement with experimental data, and but had to need a complex iteration process; (2) The L-L model (Li *et al.* 2002, 2003), which was based on the Mohr-Columb failure envelop theory, and presented the stress-strain curves using a second-order polynomial equation, and was modified and extended its application to NSC columns confined with hoop reinforcements only, or with CFRP only, or with both, and it was verified to be an accurate prediction model with easy-calculating.

Considering a concrete column wrapped by AFRP sheets, as shown in Fig. 5, the confining stress attributed to the AFRP, as given by

$$f_{1,f} = \frac{2f_f n_f t_f}{D_c} \tag{1}$$

For the RC columns, the confining stress is attributed to the hoop reinforcements, as given by

$$f_{1,s} = \frac{2f_{yv} A_{sv}}{D_{c0} s_v} \tag{2}$$

where D_c is the diameter of circular concrete column; D_{c0} is the effective diameter of circular concrete column for hoop reinforcements; and s_v is the distance of adjacent hoop reinforcements.

3.1 Lokuge model

Candappa *et al.* (2001) tested four grades of concrete (40, 60, 75 and 100 MPa) and three hydraostatic confining stresses (4, 8 and 12 MPa) and observed that the relationship curves of normalized lateral strain versus normalized axial strain had a similarity in shape regardless of the confining stress, the relationship curves of shear stress versus shear strain and the relationship curves of normalized volumetric strain versus normalized axial strain had a similar shape also. Thus, Lokuge *et al.* (2005)
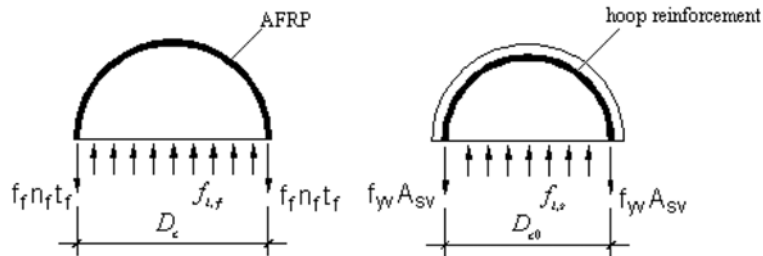

Fig. 5 Confining stress attributed to AFRP and hoop reinforcements

formulated the three relationships, and developed a prediction model based on the shear failure of concrete. When applied to RC columns, the formulas of Lokuge's model are described as follows.

$$\frac{\varepsilon_2}{\varepsilon_{cc2}} = \begin{cases} v\left(\dfrac{\varepsilon_1}{\varepsilon_{cc1}}\right) & \text{if } \varepsilon_1 \leq \varepsilon' \\[2ex] \left(\dfrac{\varepsilon_1}{\varepsilon_{cc1}}\right)^a & \text{if } \varepsilon_1 > \varepsilon' \end{cases} \tag{3}$$

$$a = 0.0177 f_{c0} + 1.2818 \tag{4}$$

$$v = 8 \times 10^{-6} (f_{c0})^2 + 0.0002 f_{c0} + 0.138 \tag{5}$$

$$\frac{\varepsilon_{cc1}}{\varepsilon_{c0}} = 1 + (17 - 0.06 f_{c0})\left(\frac{f_{l,s} + f_{l,f}}{f_{c0}}\right) \tag{6}$$

$$\frac{f_{cc}}{f_{c0}} = \left(\frac{f_{l,s} + f_{l,f}}{f_t} + 1\right)^k + \frac{f_y A_s}{f_{c0} A_0} \tag{7}$$

$$k = 1.25\left(1 + 0.062\frac{f_{l,s} + f_{l,f}}{f_{c0}}\right)(f_{c0})^{-0.21} \tag{8}$$

$$f_t = 0.9 \times 0.32 (f_{c0})^{0.67} \tag{9}$$

$$\varepsilon_{cc2} = 0.5 \varepsilon_{cc1} \tag{10}$$

$$\tau_{mp} = \frac{f_{cc} - (f_{l,s} + f_{l,f})}{2} \tag{11}$$

$$\gamma_{mp} = \frac{\varepsilon_{cc1} + \varepsilon_{cc2}}{2} \tag{12}$$

$$\sigma_1 = \begin{cases} 2\tau_{mp}(1 - e^{-c(\varepsilon_1 + \varepsilon_2)/2\gamma_{mp}}) + (f_{l,s} + f_{l,f}) \\[1ex] 2\tau_{mp}(e^{d[(\varepsilon_1 + \varepsilon_2)/2\gamma_{mp}]^2} - d) + (f_{l,s} + f_{l,f}) \end{cases} \tag{13}$$

$$c = -0.0427 f_{c0} + 7.7381 \tag{14}$$

$$d = -0.0003 f_{c0} - 0.0057 \tag{15}$$

where ε_1 and ε_2 are the axial strain and lateral strain, respectively; ε_{cc2} is the lateral strain corresponding to peak axial stress of confined concrete; ε' is the axial strain at point where shape of axial strain and lateral strain curve deviate, it can be obtained by equating the right hand side of Eq. (3); α, c, d and k are material constants; ν is the Poisson's ratio of concrete; A_s is the area of longitudinal bars; A_0 is the area of the confined concrete column; f_t is the tensile strength of concrete; τ_{mp} and γ_{mp} are the maximum shear stress and corresponding shear strain, respectively; and σ_1 is the axial stress.

Through an iterative procedure by Eq. (3) to (15) as presented by Lokuge *et al.* (2005), the complete stress-strain curves of plain and reinforced HSC circular columns confined with FRP are gained. As many researchers have pointed out, the strain measured in the confining FRP at rupture is lower than the ultimate rupture strain under pure tensile test (Lorenzi 2001, Xiao and Wu 1990). So the end condition for the Lokuge's model is that the strain of AFRP arrives 65% of the ultimate rupture strain (Xiao and Wu 2000).

3.2 L-L model

The formulas of L-L model are described as follows (Li *et al.* 2002, 2003).

$$\sigma_1 = f_{cc}\left[-\left(\frac{\varepsilon_1}{\varepsilon_{cc1}}\right)^2 + 2\left(\frac{\varepsilon_1}{\varepsilon_{cc1}}\right)\right] \tag{16}$$

$$f_{cc} = f_{c0} + f_{l,f}\tan^2\left(45° + \frac{\theta}{2}\right) + f_{l,s}\tan^2\left(45° + \frac{\theta}{2}\right) + \frac{f_y A_s}{A_0} \tag{17}$$

$$\varepsilon_{cc1} = \varepsilon_{c0}\left[1 + 2.24\tan^2\left(45° + \frac{\theta}{2}\right)\left(\frac{f_{l,f} + f_{l,s}}{f_{c0}}\right)\right] \tag{18}$$

$$\theta = 36° + 1° \times \left(\frac{f_{c0}}{35}\right) \le 45° \tag{19}$$

where θ is the angle of internal friction.

3.3 Proposed model

Fig. 4 presents that the experimental stress-strain curves are bilinear. Richard and Abbott (1975) provided a four-parameter equation for representing the bilinear curves. Fig. 6 shows the basic parameters of this equation, which is given as

$$\sigma_1 = \frac{(E_1 - E_2)\varepsilon_1}{\left[1 + \left(\frac{(E_1 - E_2)\varepsilon_1}{f_0}\right)^n\right]^{1/n}} + E_2\varepsilon_1 \tag{20}$$

where n is the curve shape parameter that mainly controls the curvature in the transition zone, for FRP confined concrete $n = 1.5\sim4$ (Almusallam 2007); f_0 is thereference plastic stress at the intercept of
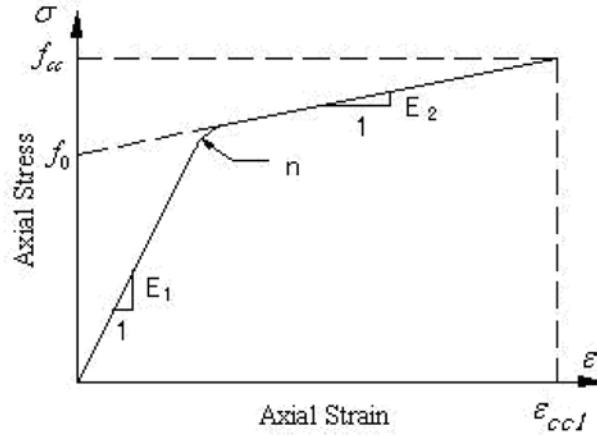
Fig. 6 Parameters of bilinear confinement model

second slope with the stress axial; E_1 is the first slope; and E_2 is the second slope, determined form the geometry of the curves as

$$E_2 = \frac{f_{cc} - f_0}{\varepsilon_{cc1}} \tag{21}$$

The above Eq. (20) has been applied to predict the complete stress-strain curves of normal-strength, high-strength, and lightweight concrete (Almusallam and Alsayed 1995) and FRP-confined plain concrete columns (Samaan *et al*. 1998, Almusallam 2007).

In order to develop a prediction model for reinforced HSC columns confined with AFRP, the confinements due to AFRP sheets and hoop reinforcements should be added up. For HSC columns confined with AFRP, the parameters (f_{cc}, ε_{cc1}, f_0, E_1 and n) maybe need redefinitions. Based on the experimental data and the previous studies (Samaan *et al*. 1998, Candappa *et al*. 2001, Lin and Liao 2004, Almusallam 2007), the simplified regression equations for f_{cc} and ε_{cc1} are as follows.

$$\frac{f_{cc}}{f_{c0}} = 1 + 3.4\frac{f_{l,f}}{f_{c0}} + 5.3\frac{f_{l,s}}{f_{c0}} + \frac{f_y A_s}{f_{c0} A_0} \tag{22}$$

$$\frac{\varepsilon_{cc1}}{\varepsilon_{c0}} = 1 + 9.5\frac{f_{l,f}}{f_{c0}} + 35\frac{f_{l,s}}{f_{c0}} \tag{23}$$

Shown in Fig. 7 are the plots of predictions from Eqs. (22) and (23) versus experimental results. There is a good consent for various concrete strength, various numbers of AFRP layers, and various ratio of hoop reinforcements.

The parameters f_0 and E_1 are given as (Samaan *et al*. 1998, ACI 1984)

$$f_0 = 0.872f_{c0} + 0.371(f_{l,s} + f_{l,f}) + f_y\frac{A_s}{A_0} + 6.258 \tag{24}$$

$$1+3.4\frac{f_{l,f}}{f_{c0}}+5.3\frac{f_{l,s}}{f_{c0}}+\frac{f_s A_s}{f_{c0} A_0}$$

(a) compressive strength

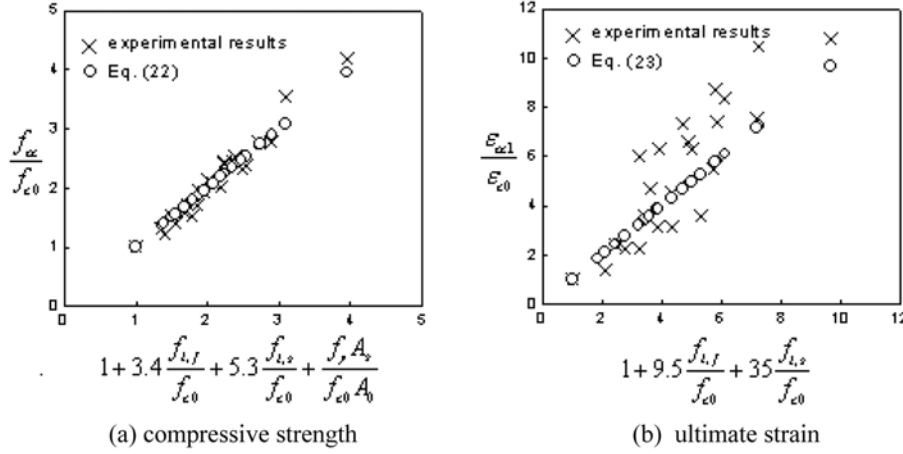$$1+9.5\frac{f_{l,f}}{f_{c0}}+35\frac{f_{l,s}}{f_{c0}}$$

(b) ultimate strain

Fig. 7 Predicted versus experimental compressive strength and ultimate strain

$$E_1 = 3320\sqrt{f_{c0}} + 6900 \tag{25}$$

Because Eq. (20) is not very sensitive to the curve shape parameter n (Samaan *et al.* 1998), a constant value 2.5 is suggested in the proposed model.

4. Comparisons of prediction models

4.1 Comparisons of compressive strength

Table 3 summarizes the experimental compressive strength and the predictions from above three models. The errors of the proposed model are between −12.49% and 17.77%, the average of absolute error is 6.12%. The errors of the Lokuge's model are between −14.29% and 14.31%, the average of absolute error is 6.51%. The errors of the L-L model are between −4.48% and 32.68%, the average of absolute error is 11.69%. It indicates that the proposed model has the best predictions, the Lokuge's model has a close accuracy as the proposed model, while the L-L model has larger deflection from the experimental results.

Some possible sources for the errors include that the regression error is always staying for the proposed model, the ultimate rupture strain of AFRP may be inaccuracy for the Lokuge's model, and the failure mode has possibly some changes for the L-L model when applying to HSC.

4.2 Comparisons of ultimate strain

Comparisons of the experimental ultimate strain and the predicted values are presented in Table 4. As mentioned by Lam and Teng (2003), the plots of ultimate strain versus confinement ratio are significant scatter, so the errors are larger. The errors of the proposed model are between −30.55% and 52.87%, the average of absolute error is 18.03%. The errors of the Lokuge's model are between −27.57% and 84.05%, the average of absolute error is 27.26%. The error of the L-L model are between −55.82% and 55.71%, the average of absolute error is 33.96%. It shows that the proposed model works better than the

Table 3 Comparison of proposed model and existing models (Compressive strength f_{cc})

Specimen designation	Experimental results f_{cc} (MPa)	Proposed model		Lokuge model (2005)		L-L model (2002,2003)	
		f_{cc} (MPa)	Error percent (%)	f_{cc} (MPa)	Error percent (%)	f_{cc} (MPa)	Error percent (%)
L-C	46.43	46.43	0.00	46.43	0.00	46.43	0.00
L-d4-1	113.91	103.23	−9.37	104.84	−7.96	108.81	−4.48
L-d4-2	163.74	143.30	−12.49	140.34	−14.29	156.89	−4.18
L-d4-3	194.71	183.36	−5.83	170.57	−12.40	204.98	5.27
M-C	78.50	78.50	0.00	78.50	0.00	78.50	0.00
M-d4-1	133.84	135.30	1.09	140.92	5.29	143.31	7.08
M-d4-2	188.66	175.37	−7.05	179.50	−4.86	193.38	2.50
M-d4-3	215.16	215.43	0.13	208.71	−3.00	243.46	13.15
M-d6-1	152.01	147.48	−2.98	150.32	−1.11	153.08	0.70
M-d6-2	197.45	187.55	−5.02	183.00	−7.32	203.15	2.89
M-d6-3	217.13	227.61	4.83	211.83	−2.44	253.22	16.62
H-C	101.18	101.18	0.00	101.18	0.00	101.18	0.00
H-d4-1	142.03	157.93	11.23	162.36	14.31	167.70	10.60
H-d4-2	193.33	198.05	2.44	203.76	5.39	219.24	13.40
H-d4-3	247.54	238.11	−3.81	235.58	−4.83	270.78	9.39
H-d6-1	160.00	170.16	6.35	173.91	8.69	177.75	11.09
H-d6-2	208.29	210.23	0.93	212.71	2.12	229.29	10.08
H-d6-3	234.86	250.29	6.57	238.15	1.40	280.83	19.57
Average (absolute error)			6.12		6.51		11.69

Table 4 Comparison of proposed model and existing models (Ultimate strain ε_{cc1})

Specimen designation	Experimental results $\varepsilon_{cc1}(\times10^{-3})$	Proposed model		Lokuge model (2005)		L-L model (2002, 2003)	
		$\varepsilon_{cc1}(\times10^{-3})$	Error percent (%)	$\varepsilon_{cc1}(\times10^{-3})$	Error percent (%)	$\varepsilon_{cc1}(\times10^{-3})$	Error percent (%)
L-C	2.55	2.55	0.00	2.55	0.00	2.55	0.00
L-d4-1	16.73	12.36	−26.11	21.90	−30.90	9.42	−43.69
L-d4-2	26.66	18.52	−30.55	26.32	−1.28	15.34	−42.47
L-d4-3	27.40	24.64	−10.06	30.14	10.00	21.25	−22.44
M-C	4.51	4.51	0.00	4.51	0.00	4.51	0.00
M-d4-1	13.81	14.73	6.63	21.29	−21.58	11.99	−55.82
M-d4-2	25.21	21.15	−16.10	25.90	−21.63	18.44	−44.21
M-d4-3	28.99	27.58	−4.87	30.06	−20.27	24.88	−34.00
M-d6-1	20.53	19.46	−5.21	27.21	32.54	13.25	−35.46
M-d6-2	24.62	25.89	5.51	31.25	26.93	19.69	−20.01
M-d6-3	33.95	32.31	−4.82	35.02	3.15	26.14	−23.01
H-C	4.56	4.56	0.00	4.56	0.00	4.56	0.00
H-d4-1	10.23	12.62	23.34	17.56	71.65	10.60	3.65
H-d4-2	19.62	17.69	−9.86	21.29	−25.90	15.81	−44.98
H-d4-3	20.07	22.71	13.16	24.73	−13.74	21.01	−26.72
H-d6-1	15.79	16.29	3.16	22.37	4.88	11.62	−45.53
H-d6-2	23.47	21.36	−9.00	25.72	−23.22	16.82	−49.79
H-d6-3	31.95	26.38	−17.43	28.90	−27.57	22.02	−44.80
Average (absolute error)			18.03		27.26		33.96

others. Excepting aforementioned scatter, these errors maybe caused by the neglect of attribution due to the longitudinal bars.

4.3 Comparisons of stress-strain curve

In Figs. 8~10, the experimental axial stress-strain curves are compared with three theoretical curves calculated from the proposed model, the Lokuge's model and the L-L model. Each experimental curve is one among the three curves of each type of specimens,

It can be observed that

1. The proposed model and the Lokuge's model provide distinctly bilinear stress-strain curves, which are the basic character of the experimental curves. The L-L model, however, provides parabolic curves that violate the experimental observation.
2. For the most of specimens, the L-L model can predict the starting stage better, but the proposed model and the Lokuge's model can predict the second stage better.
3. When the concrete strength is lower, as Fig. 8 shows, the differences between the proposed model
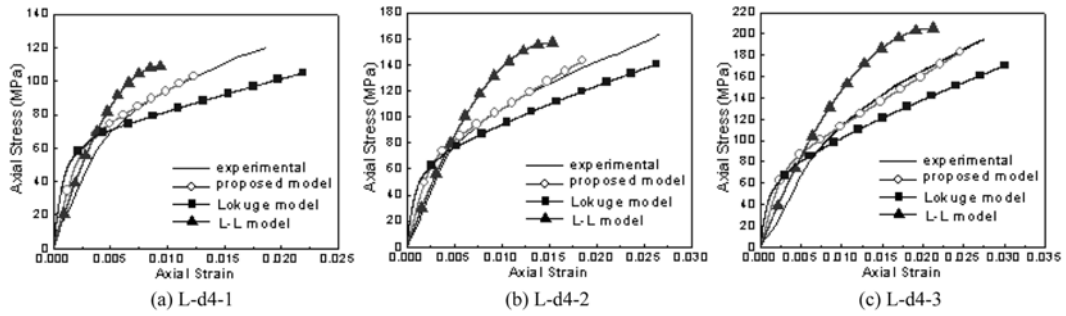

Fig. 8 Comparison of experimental stress-strain curves with predictions of the prediction models (f_{c0} = 46.43 MPa)
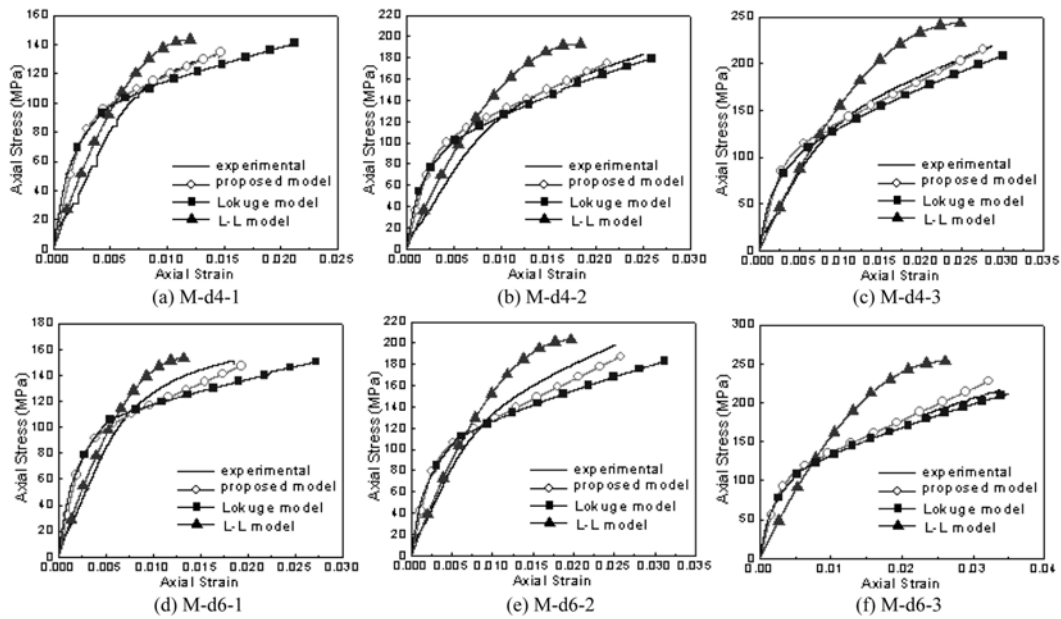

Fig. 9 Comparison of experimental stress-strain curves with predictions of the prediction models (f_{c0} = 78.50 MPa)
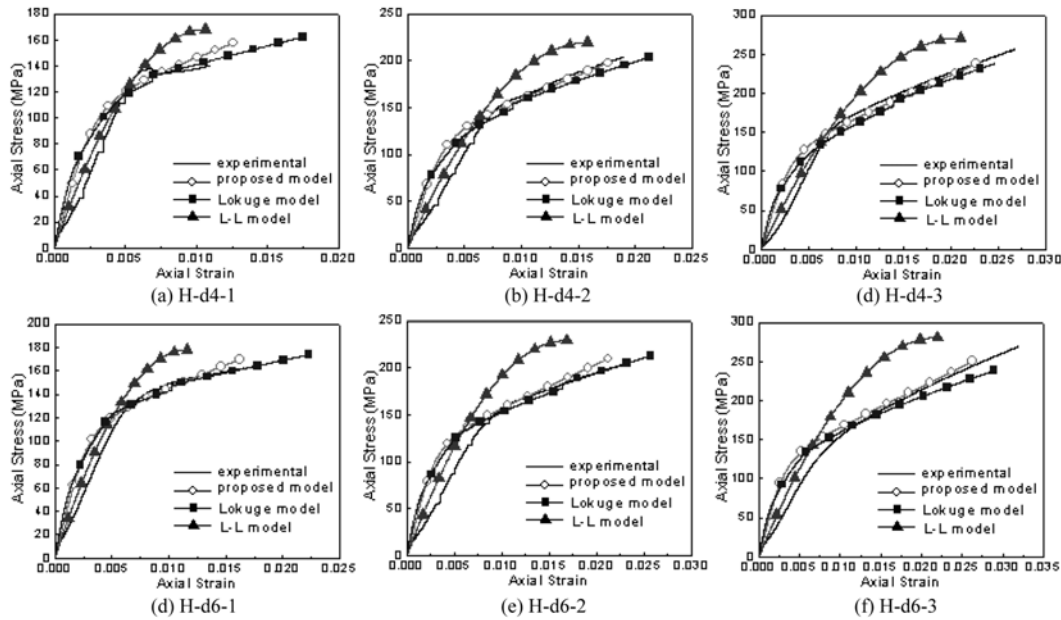
Fig. 10 Comparison of experimental stress-strain curves with predictions of the prediction models (f_{c0} = 101.18 MPa)

and the Lokuge's model are large, the former are closer to experimental curves. When the concrete strength is higher, as shown in Fig. 9 and Fig. 10, the differences between them are small, they are both agree with the experimental results well.

Through the above comparisons, it is demonstrated that the proposed model and the Lokuge's model are adapted to the stress-strain curves predictions for high-strength circular reinforced concrete columns confined by AFRP. However, considering convenience in calculation, the proposed model is better.

5. Conclusions

1. The phenomena of crushed concrete, which appeared when the specimens were failed completely, indicate that the brittleness of HSC could be improved by the confinement due to AFRP sheets and hoop reinforcements.
2. The compressive strength and the ultimate strain of AFRP-confined reinforced HSC short columns can be increased notably. For the same grade of concrete strength, there are more increments with more amount of AFRP wrapping. When the same amount of AFRP applied, the increments are reduced relatively as the strength of concrete increasing because HSC is more brittleness as its strength increasing.
3. All the experimental axial stress-strain curves are bilinear consisted of two stages. In the first stage, the specimens behave similarly as the unconfined columns. In the second stage, after arriving the unconfined strength, the curves ascended with reduced slopes.
4. Based on the experimental results, a prediction model has been proposed in this paper. Comparing with the experiments results and predictions from two existing models (the Lokuge's model and

the L-L model), it is demonstrated that the proposed model can provide better accurate predictions in the subjects of compressive strength, ultimate strain, and stress-strain curves.

Acknowledgments

Notations

The following symbols are used in this paper

A_0	area of the confined concrete column (mm^2)
A_s	area of longitudinal reinforcement (mm^2)
A_{sv}	area of hoop reinforcements (mm^2)
d_{sv}	diameter of hoop reinforcements (mm)
D_c	diameter of circular concrete column (mm)
D_{c0}	effective diameter of circular concrete column for hoop reinforcements (mm)
E_f	elastic modulus of AFRP (MPa)
E_s	elastic modulus of longitudinal reinforcement (MPa)
E_{sv}	elastic modulus of hoop reinforcements (MPa)
E_1	the first slope of stress-strain curve, in the proposed model (MPa)
E_2	the second slope of stress-strain curve, in the proposed model (MPa)
f_{cc}	compressive strength (peak axial stress) of confined concrete column (MPa)
f_{c0}	strength of unconfined concrete (MPa)
f_f	tensile strength of AFRP
$f_{l,f}$	confining stress due to AFRP
$f_{l,s}$	confining stress due to hoop reinforcements (MPa)
f_t	tensile strength of concrete (MPa)
f_{yv}	yield strength of hoop reinforcements (MPa)
f_y	yield stress of longitudinal reinforcement (MPa)
f_0	reference plastic stress at the intercept of second slope with the stress axis (MPa)
n	curve shape parameter
n_f	number of AFRP layer
s_v	distance of adjacent hoop reinforcements (mm)
t_f	thickness of AFRP (mm)
α, c, d, k	material constants in the Lokuge's model

ε_{cc1} axial strain corresponding to f_{cc} (m/m)

ε_{cc2} lateral strain corresponding to f_{cc} (m/m)

ε_{c0} axial strain at f_{c0} (m/m)

ε_{fu} ultimate rupture strain of AFRP

ε_{l} axial strain (m/m)

ε_{2} lateral strain (m/m)

ε' axial strain at point where shape of axial strain and lateral strain curve deviate, in the Lokuge's model (m/m)

ν Poisson's ratio

τ_{mp} maximum shear stress (MPa)

γ_{mp} shear strain corresponding τ_{mp} (m/m)

σ_{l} axial stress (MPa)

θ angel of internal friction

ϕ strength-reduction factors

References

Almusallam, T.H. (2007), "Behavior of normal and high-strength concrete cylinders confined with E-glass/epoxy composite laminates", *Compos. Part B-Eng.*, **38**(5-6), 629-639.

Almusallam, T.H., and Alsayed, S.H. (1995), "Stress-strain relationship of normal, high-strength and lightweight concrete", *Mag. Concrete. Res.*, **47**, 39-44.

American Concrete Institute (1984), "State of the art report of high-strength concrete", *ACI 363R-84*, ACI-363 Committee, Detroit.

Candappa, D.P., Sanjayan, J.G. and Setunge, S. (2001), "Complete triaxial stress-strain curves of high-strength concrete", *J. Mater. Civil. Eng.*, **13**(3), 209-215.

Fam, A. Z. and Rizkalla, S.H. (2001), "Confinement model for axially loaded concrete confined by circular fiber-reinforced polymer tubes", *ACI Struct. J.*, **98**(4), 451-461.

Karabinis, A.I. and Rousakis, T.C. (2002), "Concrete confined by FRP materials: a plasticity approach", *Eng. Struct.*, **24**(7), 923-932.

Lam, L. and Teng, J.G. (2002), "Stress-strain model for FRP-confined concrete", *Constr. Build. Mater.*, **17**, 471-489.

Li, Y.F., Lin, C.T. and Sung, Y.Y. (2002), "A constitutive model for concrete confined with carbon fiber reinforced plastics", *Mech. Mater.*, **35**(3-6), 603-619.

Li, Y.F., Fang, T.S. and Chern, C.C. (2003), "A constitutive model for concrete cylinder confined by steel reinforcement and carbon fiber sheet", *Proceedings of Pacific Conference on Earthquake Engineering*, New Zealand, Feb.

Li, G.Q. (2006), "Experimental study of FRP confined concrete cylinders", *Eng. Struct.*, **28**(7), 1001-1008.

Lin, H.J. and Liao, C.I. (2003). "Compressive strength of reinforced concrete column confined by composite material", *Compos. Struct.*, **65**(2), 239-250.

Lin, H.J., Liao, C.I. and Yang, C. (2006), "A numerical analysis of compressive strength of \r\nrectangular concrete columns confined by FRP", *Comput. Concrete*, **3**(4), 57-68.

Lokuge, W.P., Sanjayan, J.G. and Setunge, S. (2005), "Stress-strain model for laterally confined concrete", *J. Mater. Civil. Eng.*, **17**(6), 607-616.

Lorenzis, L.D. (2001), "A comparative study of models on confinement of concrete cylinders with FRP composites", Research Rep. Prepared of Chalmers Univ. Of Technology, Goteborg, Sweden.

Mirmiran, A. and Shahawy, M. (1997), "Behavior of concrete columns confined by fiber composites", *J. Struct. Eng.*, **123** (5), 583-590.

Mortazavi, A.A., Pilakoutas, K. and Son, K.S. (2003), "RC column strengthening by lateral pre-tensioning of

FRP", *Constr. Build. Mater.*, **17**(6-7), 491-497.

Richard, R.M. and Abbott, B.J. (1975), "Versatile elastic-plastic stress-strain formula", *J. Eng. Mech.*, **101**(4), 511-515.

Saafi, M., Toutanji, H.A. and Li, Z. (1999), "Behavior of concrete columns confined with fiber reinforced polymer tubes", *ACI Mater. J.,* **96**(4), 500-509.

Samaan, M., Mirmiran, A. and Shahawy, M. (1998), "Model of concrete confined by fiber composites", *J. Struct. Eng.*, **124**(9), 1025-1031.

Tabash, S.W. (2007), "Stress-strain model for high-strength concrete confined by welded wire fabric", *J. Mater. Civil. Eng.*, **19**(4), 286-294.

Teng, J.G., and Lam, L. (2004), "Behavior and modeling of fiber reinforced polymer-confined concrete", *J. Struct. Eng.*, **130**(11), 1731-1723.

Xiao, Y. and Wu, H. (2000), "Compressive behavior of concrete confined by carbon fiber composite jackets", *J. Mater. Civil. Eng.*, **12**(2), 139-146.

Yeh, F.Y. and Chang, K.C. (2007), "Confinement efficiency and size effect of FRP confined circular concrete columns", *Struct. Eng. Mech.*, **26**(2), 127-150.

CC